Ionization suppression in a very-short-range potential

A. Sanpera
Departament de Física, Universitat Autònoma de Barcelona, 08193 Bellaterra, Spain

Q. Su*
Department of Physics and Astronomy, University of Rochester, Rochester, New York 14627

L. Roso-Franco
Departamento de Física Aplicada, Universidad de Salamanca, 37071 Salamanca, Spain
(Received 6 April 1992)

We study numerically the photoionization of a one-dimensional model atom, with a very-short-range potential, in the Kramers-Henneberger frame. In the range where suppression of ionization is found, the ground-state depletion follows a well-fitted exponential decay. The decay rate has been examined for different values of the laser frequency and for different intensities. Comparisons with existing analytical predictions are made where appropriate.

PACS number(s): 32.80.Rm, 42.50.Hz

I. INTRODUCTION

Our knowledge of atomic ionization processes under strong radiation fields is still incomplete. When the radiation field strength is comparable to the typical atomic Coulomb field strength, we enter a new region where numerical simulations are a fundamental tool in understanding the underlying physical effects. Very recently, numerical solutions of the Schrödinger equation have been important in advancing our understanding of certain unexpected effects such as ionization suppression (atomic stabilization) and electron localization by very short laser pulses [1–10]. Ionization suppression, or atomic stabilization, means that the ionization rate becomes a decreasing function of the laser intensity. Both stabilization of the population in Rydberg levels [6,11,12] and stabilization of atoms in the ground state [9,10] have been described in quantum-mechanical theories, and discussions of stabilization based on classical Newtonian equations have also been presented [8,13].

In some cases it has been reported that the residual ionization in the stabilization regime is quite slow, with well-defined linear rates [4]. Analytical expressions to predict these slow ionization rates are just beginning to be reported [14–17]. Few laboratory experiments related to stabilization phenomena are in progress [18]. Therefore we consider that numerical tests of these analytical predictions are desirable.

In the original formulation of stabilization theory, developed by Gersten and Mittleman [19] and Gavrila and co-workers [20,21], a laser field of asymptotically high frequency and high intensity was assumed. They showed that, under such conditions, the atom remains stable against both ionization and bound-state–bound-state transitions because the Hamiltonian that describes the system (including the field-atom interaction) is well represented as being time independent in a convenient reference frame. This is the time-averaged Kramers-Henneberger coordinate frame [22,23]. In this frame the entire atom-field interaction is exactly converted to a time-dependent shift of the argument of the atomic potential. For a sufficiently-high-frequency laser field, the oscillating potential can be replaced by its time average, which is a function with two minima instead of one. For a sufficiently high intensity, the ground state of this new potential is represented by an electronic wave function clearly localized near the positions of these two wells, an effect often referred to as dichotomy. The Kramers-Henneberger picture has been used very directly, for example, for the interpretation of atomic stabilization and electron localization in electron wave-packet calculations for one spatial dimension by Su *et al.* [1,3], Reed and Burnett [7], Reed, Knight, and Burnett [5], and Kulander, Shafer, and Krause [9] for three spatial dimensions.

The observation of slow ionization raised again the question of whether a modified perturbation approach can still be efficient in understanding the physics in an intense-field domain. So far there are only a few analytical theories bearing on the question of ground-state stabilization. They are generally restricted in validity by the use of some form of perturbation theory and the assumption of asymptotically high frequency. Attempts based on this idea have been applied in analyzing simple models. These analyses were argued to be accurate for asymptotically high frequencies, while the question remains as to how effective they are in the moderate high frequencies. By moderate high frequency we mean here photon energies comparable to the atomic ionization potential.

In this paper we present a relatively simple numerical model for strong-field laser-atom dynamics. We will deal with a one-dimensional atomic model and we will consider a very-short-range potential. In fact, a short-range potential represents the photodetachment of an electron from a model negative ion [24] rather than the ionization

of a neutral atom. Our very-short-range potential can be considered as a reasonable introductory approach to the study of negative ions. The advantage of this model is that it has been analytically studied by other authors [15,16], so it represents a good test to understanding the relevant mechanisms leading to stabilization. Moreover, by studying the photodetachment dynamics for this model we will find for certain regime rather simple empirical expressions for the residual probability defining the electron still in a bound state after the pulse.

We will consider only the nonrelativistic problem, although for the upper limit of the intensities considered in this paper this assumption can be questioned. The interaction Hamiltonian is considered in the electric dipole approximation. The laser field will be taken in the form

$$E(t)=\mathcal{E}f(t)\sin\omega t \ , \tag{1}$$

where $f(t)$ is a pulse-shape function with unit amplitude, and $\mathcal{E}$ is the peak field strength. In this paper we calculate the time evolution of the electron's wave function numerically in the Kramers-Henneberger frame. In this approach, the relevant parameter of the theory is α_0, the classical excursion amplitude of a free electron in an oscillating external field with peak field strength $\mathcal{E}$ and frequency ω

$$\alpha_0=e\mathcal{E}/m\omega^2=\mathcal{E}/\omega^2 \tag{2}$$

(in atomic units). We have monitored the ionization process by analyzing the depletion of the ground-state population. For a wide range of frequencies and laser intensities ($0.25<\omega<1.41$ a.u., $1.3\times10^{16}<I<9\times10^{20}$ W/cm^2), we have found depletion to be well represented by a pure exponential decay.

We present a survey of the decay rate considered as a function of both α_0 and ω. We show that the decay rate appears to follow simple scaling laws. We compare these scaling laws with the analytical predictions done by Grozdanov, Krstic, and Mittleman [15]. We have verified that for a large range of field parameters the scaling relations hold very well. The numerically found values of these rates are more than one order of magnitude smaller than these recent analytical predictions. Nevertheless, we have been able to identify the origin of this discrepancy.

II. DESCRIPTION OF THE MODEL

The very-short-range atomic potential is mathematically represented by a Dirac δ function [25,26]. In the usual reference frame, the laboratory frame, the Hamiltonian that describes the evolution of the electron is, using dipole approximation,

$$i\frac{\partial}{\partial t}\psi(x,t)=\left[-\frac{1}{2}\frac{\partial^2}{\partial x^2}-g\delta(x)-xE(t)\right]\psi(x,t) \ . \tag{3}$$

here and throughout this paper we adopt atomic units, for which $m=e=\hbar=1$.

Before the field is turned on, $t<0$, the electron is bound by the δ-function potential and the bare ground-state wave function is

$$\psi(x,t)=\sqrt{g}\,e^{-g|x|}e^{-iE_0t} \ , \tag{4}$$

where $E_0=-g^2/2$ is the bound-state energy and $g>0$ is the strength of the δ-function potential. However, this state will not be the initial state in our computations. Our interest is in the nature of the photodetachment process at a given intensity, and we will neglect all practical complications arising from the turn-on of the laser pulse. Thus we will assume that the atom is initially prepared in the corresponding Kramers-Henneberger ground state, a condition assumed also in the theoretical work with which we will compare our results.

By doing so we are not able to answer the question about the degree of stabilization. Instead we study the residual ionization rate once the atom or negative ion survives a smooth turn-on of the laser pulse. Clear evidence from other simulations [4] suggests that having a significant fraction of the population pumped into very few Kramers-Henneberger eigenstates just after the turn-on is a reasonable assumption.

The Schrödinger equation in the Kramers-Henneberger (KH) picture is well known to take the form [22]

$$i\frac{\partial}{\partial t}\psi_{\rm KH}(x,t)=\left[-\frac{1}{2}\frac{\partial^2}{\partial x^2}+V(x+\alpha(t))\right]\psi_{\rm KH}(x,t) \tag{5}$$

and the time dependence is now included in the Kramers-Henneberger potential

$$V(x+\alpha(t))=-g\delta(x+\alpha(t)) \ , \tag{6}$$

where

$$\alpha(t)=-\int dt''\int E(t')dt'=\alpha_0 f(t)\sin\omega t \ . \tag{7}$$

Obviously the second equality holds for $f(t)=1$, but it is also true whenever $f(t)$ is a very smooth function of the time. The classical excursion amplitude α_0 was defined in (2).

It is easier to solve the Schrödinger equation in the Kramers-Henneberger frame (5) than in the laboratory frame (3). In the former case, only the points between $+\alpha_0$ and $-\alpha_0$ contribute to the potential, while in the latter case the electric dipole interaction term is unbound for large $|x|$.

To be more precise about the meaning of the Kramers-Henneberger eigenstates, which is necessary at the initial time of our calculation, we make a Fourier-Floquet expansion of the potential (6)

$$V(x+\alpha(t))=\sum_{n=-\infty}^{\infty}V_n(x,\alpha_0)e^{-in\omega t} \ , \tag{8}$$

where the coefficients of the expansion are

$$V_n(x,\alpha_0)=\frac{1}{2\pi}\int_{-\pi}^{+\pi}V(x+\alpha(\varphi))e^{in\varphi}d\varphi \ , \quad \varphi=\omega t \ . \tag{9}$$

Now we neglect, as usual, all the terms except for the cycle average of the Kramers-Henneberger potential. This is obviously better justified the greater the laser frequency compared to the characteristic frequency of the ground state of the system in this frame. This is the origin of the

asymptotic assumption made in the earliest treatments. The surviving term reads

$$V_0(x,\alpha_0)=-\frac{g}{2\pi}\int_{-\pi}^{+\pi}\delta(x+\alpha(\varphi))d\varphi$$
$$=\begin{cases}-\dfrac{g}{\pi(\alpha_0^2-x^2)^{1/2}}\ , & |x|\le|\alpha_0| \\ 0\ , & |x|>\alpha_0|\ .\end{cases} \tag{10}$$

This new potential $V_0(x,\alpha_0)$, the so-called "dressed" potential, has of course an area equal to g. Here and throughout we will consider $g=1$, to work in an energy regime similar to that of the electron in a hydrogen atom (the energy of the bare ground state, in the laboratory frame, is $-g^2/2=-0.5$ a.u.). The dressed potential has been depicted in Fig. 1. If $\alpha_0>0$ it always presents this two minima structure.

The solutions of the time-independent Schrödinger equation of the dressed atom in the Kramers-Henneberger frame,

$$\left[-\frac{1}{2}\frac{\partial^2}{\partial x^2}+V_0(x,\alpha_0)\right]\Phi^n_{\rm KH}(x)=E^n_{\rm KH}\Phi^n_{\rm KH}(x)\ , \tag{11}$$

can be obtained using standard numerical techniques, and the only two points that need some special consideration are the two singularities at $x=\pm\alpha_0$ [27]. These eigenfunctions form a complete set of states. As usual, the wave function is

$$\psi_{\rm KH}(x,t)=\Phi_{\rm KH}(x)e^{-iE_{\rm KH}t}\ , \tag{12}$$

where the quantum number specifying each state is omitted. Equation (11) cannot be worked out analytically. Some approximate solutions have been reported [16]. These were obtained by replacing the static dressed potential $V_0(x,\alpha_0)$ by an approximated dressed potential with two δ functions at the singularities ($x=\pm\alpha_0$), properly normalized in order to preserve the original area. Although the singularities are fairly well represented by the δ functions, the approximation will work correctly only for asymptotically high values of α_0. Moreover, the number of eigenstates that can be supported by two δ-function potentials in one dimension is equal to 2. However, the true Kramers-Henneberger version of a δ-function potential can support a finite number of bound eigenstates, and the number of bound eigenstates increases with α_0. Therefore we solve numerically Eq. (11) without introducing approximations.

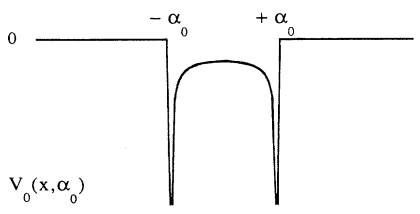

FIG. 1. The static dressed potential $V_0(x,\alpha_0)$ in the Kramers-Henneberger frame.

We have sought the eigenvalues and eigenfunctions of the bound states of the Kramers-Henneberger static potential for α_0 ranging from 0 to 100 a.u. It corresponds to the interval of laser intensities that we will study in our simulations. We find from one to six bound states depending on the value of α_0. The results are plotted in Fig. 2, where we can see the energies of the bound states for different values of α_0. As the potential is central, parity is a good quantum number, and the eigenstates are even or odd.

The behavior of the eigenvalues is clear. For very small α_0 this Kramers-Henneberger potential has only one bound state with even parity which is very similar to the bare potential ground state. When α_0 increases, the ground state begins to be able to reflect the two-well structure of the potential. Then it starts to present a typical structure with two maxima around $x=\pm\alpha_0$ and a minimum close to $x=0$ (dichotomy of the wave function). Increasing α_0 larger than about 8 a.u., a new bound state, of odd parity, appears. Because of the parity of this new state, at $x=0$ its wave function vanishes. As α_0 increases, the dichotomy of the ground-state wave function is more clear and therefore its amplitude at $x=0$ is smaller. This implies that for very large α_0, $\alpha_0>50$ a.u., these two bound states are effectively degenerated. Finally, pairs (even-odd) of quasidegenerate states are found at large α_0.

We have also analyzed the behavior of the ground state as a function of the classical excursion amplitude α_0. Dichotomy start to be significant for relative small α_0 values ($\alpha_0>5$ a.u.). Even so, for small α_0, the two singularities of the potential are so close that the mutual influence is important. Only for values of $\alpha_0\ge 50$ a.u. are there simple scaling laws for the ground-state energy $|E_0(\alpha_0)|$ and a scaling law for the ground-state wave function at the "return" points $|\Phi(\alpha_0)|$:

$$|E_0(\alpha_0)|\propto\alpha_0^{-2/3}\ , \tag{13}$$

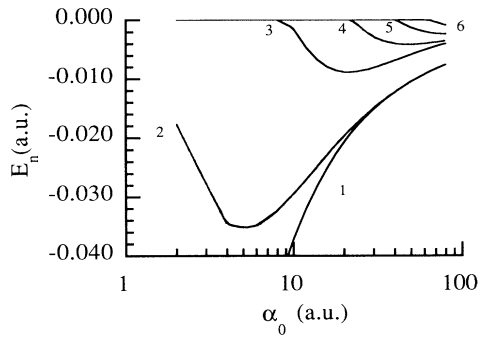

FIG. 2. Eigenvalues of the static dressed potential in the Kramers-Henneberger frame, as a function of α_0. As α_0 increases, quasidegenerate pairs of odd-even wave functions appear. Even states ($n=1,3,5$) and odd states ($n=2,4,6$) are indicated by the quantum number n, being $n=1$ the ground state. The bare ground state (the bound state for $\alpha_0=0$) lies far below the window of this drawing (it is the end of the continuous line $n=1$ that goes down as α_0 decreases).

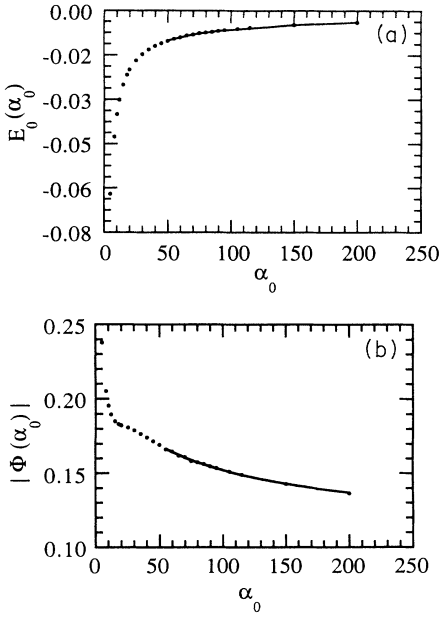

FIG. 3. (a) Ground-state energies, and (b) ground-state wave function at $x=\alpha_0$ of the static potential in the Kramers-Henneberger frame as a function of α_0. Dots represent numerical computation. Continuous lines represent the fit, according to Eqs. (13) and (14), for $\alpha_0 > 50$ a.u.

$$|\Phi(\alpha_0)| \propto \alpha_0^{-1/6} . \tag{14}$$

Our results are summarized in Fig. 3. In Fig. 3(a) we have represented the ground-state eigenvalue as a function of α_0. The range in which scaling is possible has also been fitted by expression (13). The same argument is repeated for the value of the ground state at the return points in Fig. 3(b). These scalings agree with those indicated in the work of Grozdanov, Krstic, and Mittleman [15].

For the time-dependent regime we solve Eq. (5) by discretizing all the operators and using a Crank-Nicholson algorithm. The parameters that characterize the grid are strongly dependent on the intensity and the frequency used. In order to better represent the dressed potential, we must use a large number of points between $x=\pm\alpha_0$. The grid has a length of 2000 a.u. (20 001 points).

The field is always represented by a square pulse of 30 optical cycles. Therefore a pulse-shape function $f(t)=1$, for $0 \geq t \geq 60\pi/\omega$ and $f(t)=0$, before and after, is considered. We always consider that the electron is initially prepared in the Kramers-Henneberger ground state corresponding to the intensity of the pulse. This initial condition, instead of the electron's bare ground state, simplifies the turn-on process, agrees partially with other more detailed studies of the turn-on, and allows us to concentrate on the dynamics of stabilization.

Like in the case of long-range potentials [4], we found that initial state population remained steady in the Kramers-Henneberger frame throughout the pulse, and no significant excitation to excited levels took place. This may be considered as evidence in favor of the perturbative treatment from the Kramers-Henneberger ground state. For the case of a frequency $\omega=0.5$ a.u., with a square pulse of 30 optical cycles and for different values of the amplitude, ranging from $\mathcal{E}=2$ to 20 a.u. ($I=2.2\times10^{17}-1.4\times10^{19}$ W/cm^2), we have seen that the total population in the excited bound states is remarkably small. The main contribution to the ionized population is made by ground-state depletion directly. In Fig. 4 we have plotted the total ionized population as well as all the bound-state populations for a square pulse of frequency

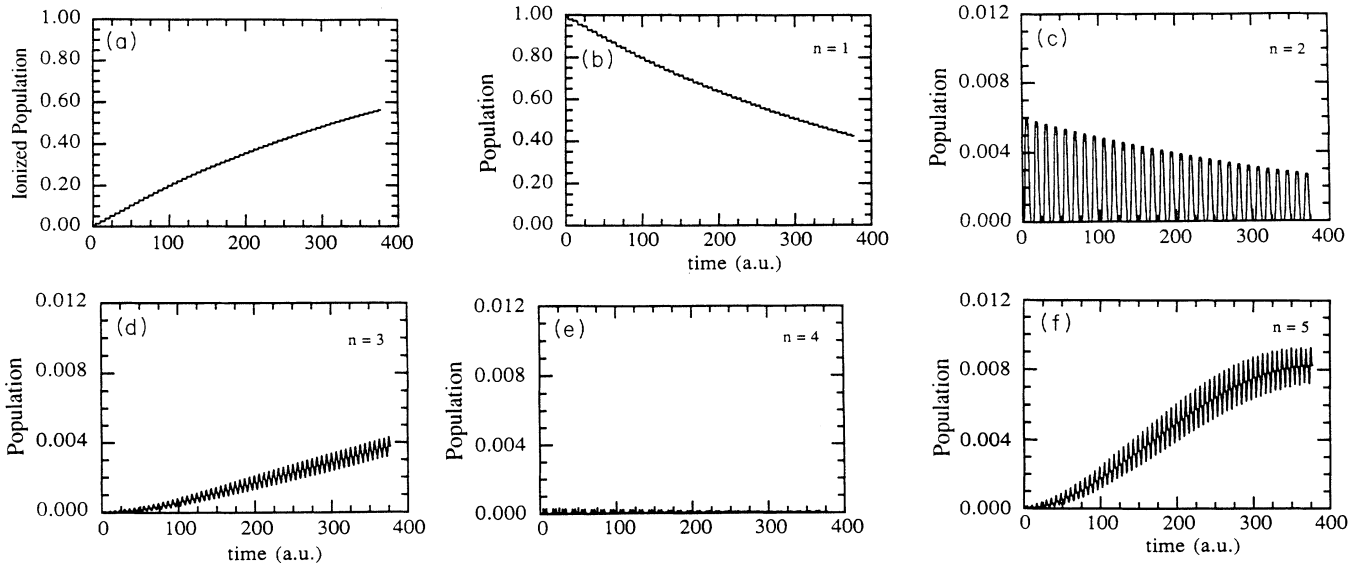

FIG. 4. Time dependence of the population ionized and of the populations of the five bound states existing for $\alpha_0=60$ a.u. It corresponds to a square pulse of frequency $\omega=0.5$ a.u. $n=1$, 3, and 5 are the even bound states, $n=1$ being the ground state. $n=2$ and 4 are the odd bound states.

$\omega=0.5$ a.u. and $\alpha_0=60$ a.u. The effect of considering the population of all the excited bound states will change the total ionization population by an amount less than 2×10^{-3}.

III. COMPUTED DETACHMENT RATES

We define the detached population as usual:

$$P_{\text{ion}}=\int|\langle\psi_{\text{KH}}(x,t)|u^k_{\text{KH}}(x)\rangle|^2dk$$
$$=1-\sum_n|\langle\psi_{\text{KH}}(x,t)|\Phi^n_{\text{KH}}(x)\rangle|^2\ , \tag{15}$$

where $u^k_{\text{KH}}(x)$ and $\Phi^n_{\text{KH}}(x)$ are the free (positive-energy) eigenstates and bound eigenstates in the Kramers-Henneberger frame. Because the number of bound states is always finite, and not large for this potential, the second form of Eq. (15) is easier to calculate.

Rather than keeping our attention on the detached population, let us now consider the ground-state depletion, which is mainly responsible for the dynamics. What we obtain, as shown in Fig. 5, is a very-well-fitted exponential decay (for each value of α_0 and ω). This allow us to define in a unique way the decay rate of the process, so we can write the time dependence of the Kramers-Henneberger ground-state population as

$$P_{\text{ground}}(t)=P_{\text{ground}}(0)e^{-\Gamma(\alpha_0,\omega)t}\ . \tag{16}$$

In order to know the dependence of the decay rate Γ on α_0 and ω, we have obtained the ionization rate for four different laser frequencies ($\omega=0.25$, 0.5, 1, and 1.41 a.u.) and a wide range of values of α_0 (from 10 to 80 a.u.). This corresponds to a huge range of intensities, between 3.5×10^{16} and 9×10^{20} W/cm^2 which are mostly still far away from experimental parameters now available. Except for the case $\omega=0.25$ a.u., the lowest frequency studied, we have considered the square pulse only of 15 optical cycles instead of the standard 30 optical cycles.

If we plot the decay rate versus α_0, as in Fig. 6, it is clear that the behavior within a large range of α_0's and ω's is well described by a straight line. From now on we will constrain ourselves to this regime. On the other hand, a careful analysis of the rates Γ associated with each frequency, for a constant α_0, leads us to a simple empirical relationship

$$\omega_1\times\Gamma(\omega_1)\simeq\omega_2\times\Gamma(\omega_2)\ . \tag{17}$$

Therefore we can suggests a simple empirical expression for the decay rate in this range of values of both intensity

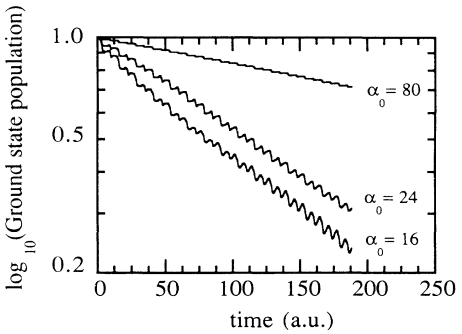

FIG. 5. Ground-state depletion, in logarithmic scale, vs time. It corresponds to a square pulse of frequency $\omega=0.5$ a.u. and several values of α_0. One can observe that the decay is well associated with a pure exponential.

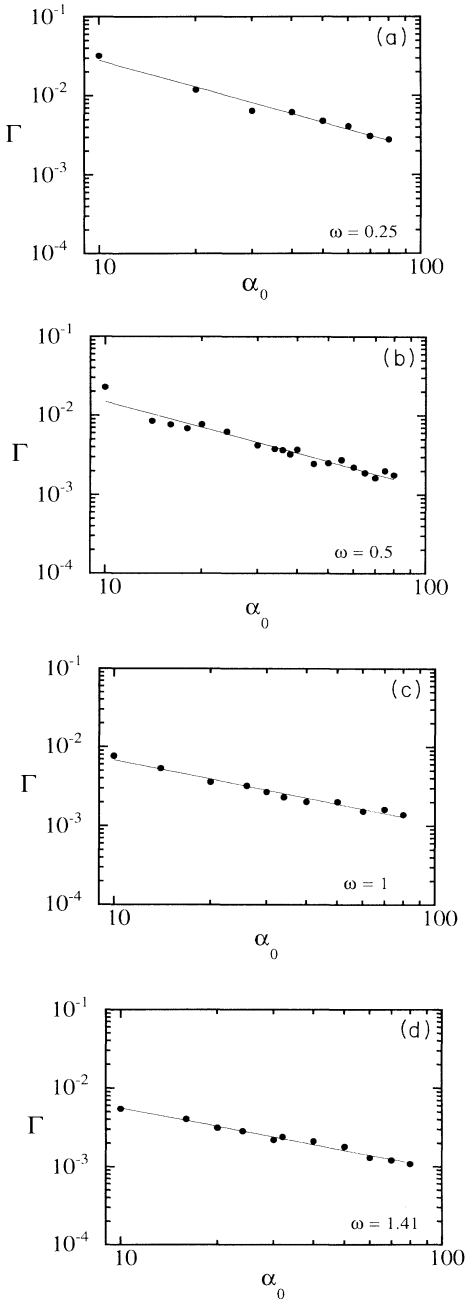

FIG. 6. Ground-state decay rate Γ vs the electron's classical excursion amplitude α_0 (both in atomic units) for four different values of the laser frequency, $\omega=0.25$, 0.50, 1, and 1.41 a.u., calculated from the numerical simulation (dots). These dots have been then fitted by a straight line in each case, according to Eq. (18).

and frequency:

$$\Gamma(\alpha_0,\omega)\simeq A_1(\omega)+\frac{A_2}{\omega\alpha_0}\ , \tag{18}$$

where A_2 is found to be close to a constant ($A_2=0.07$ a.u.) We do not have enough data to get an accurate expression for $A_1(\omega)$, but its contribution to expression (18) is always smaller than the term proportional to A_2. We will neglect the $A_1(\omega)$ term in this paper and focus on the validity of a detachment rate inversely proportional to $\omega\alpha_0$.

There is a restriction on the parameters α_0 and ω corresponding to this ionization regime inversely proportional to $\omega\alpha_0$. The restriction amounts to the satisfaction of the inequality $\alpha_0\omega\geq 10$ a.u. This product is the amplitude of the classical velocity of the electron in the field. This restriction can be interpreted as follows. First, we understand that ionization is possible only when the laser field and the binding potential act together. Neither is adequate by itself. In the Kramers-Henneberger frame the oscillations of the binding potential past the (almost stationary) electron are relatively rapid and the electron only spends an amount of time

$$\Delta T\approx\Delta x_0/v\approx 1/(\omega\alpha_0) \tag{19}$$

in the vicinity the potential every cycle. Thus there is only a probability $P_{\text{decay}}\approx\Gamma\Delta T$ that the electron becomes ionized every cycle. Now we can apply (18) and evaluate this probability:

$$P_{\text{decay}}\approx\frac{A_2}{\omega^2\alpha_0^2} \tag{20}$$

(per cycle). For velocities above the "critical" value $v\approx 10$ a.u. we are safely in the regime where ionization occurs with negligible probability ($P_{\text{decay}}<10^{-3}$) during a typical encounter of the electron and the potential. Below this critical value of velocity we enter into another regime of ionization where the overlap time during an encounter is long enough for ionization to be significant.

IV. COMPARISON WITH ANALYTICAL PREDICTIONS

Now we will compare our numerical results of the ground-state decay with the predicted rate found in the literature [15,17]. For this potential, and assuming that the frequency of the process is high enough so that the final state is considerable as a plane wave, the properly normalized decay rate is given by

$$\Gamma=\frac{2|\Phi(\alpha_0)|^2}{\pi^2\omega\alpha_0}\sum_{n=1}^{\infty}\frac{1}{n}[1+(-1)^n\sin(2\alpha_0\sqrt{2n\omega})] \tag{21}$$

after imposing the condition that $q_n\alpha_0\gg n$, where q_n is the final momentum of the electron ($q_n=\sqrt{2n\omega}$). The main difficulty in evaluating this expression comes from the lack of knowledge of the initial wave function. Grozdanov, Krstic, and Mittleman [15] used some approximations for the initial wave function that allows to reduce the above expression to

$$\Gamma=\frac{\Gamma^{(0)}}{\omega\alpha_0^{4/3}}\ln(2\omega\alpha_0^2)\ , \tag{22}$$

where $\Gamma^{(0)}$ is of the order of unity and independent of ω and α_0. Our numerical results show good agreement with the general behavior of expression (22), but very poor agreement with the numerical values of the width. Our numerical rates are approximately one order of magnitude smaller than those predicted by expression (22); in other words, our rate fits (22) for $\Gamma^{(0)}\simeq 1/35$ a.u. For this reason, instead of making some approximations on the dressed potential and therefore on the initial wave function, we directly use the computed values of $|\Phi(\alpha_0)|^2$ already showed in Fig. 3(b) to evaluate the width through expression (21). Then we compare it with the results obtained from the ground-state decay plots. In this range of parameters ($10\leq\alpha_0\leq 100$ a.u. and $0.25\leq\omega\leq 1.41$ a.u.) a good fit with the behavior α_0^{-1} is also suitable without contradicting the $\alpha_0^{-4/3}$ behavior of Eq. (22). In Fig. 7(a), we plot the analytical prediction (21) for the range of parameters tested in our numerical simulations. We have included the linear fit of these data in order to better compare with our the numerical results, which are repeated in Fig. 7(b) at the same scale and also with the linear fit. Actually, the agreement between both results—expressions (18) and (21)—is quite good, taking into account the approximations made in the analytical calculation.

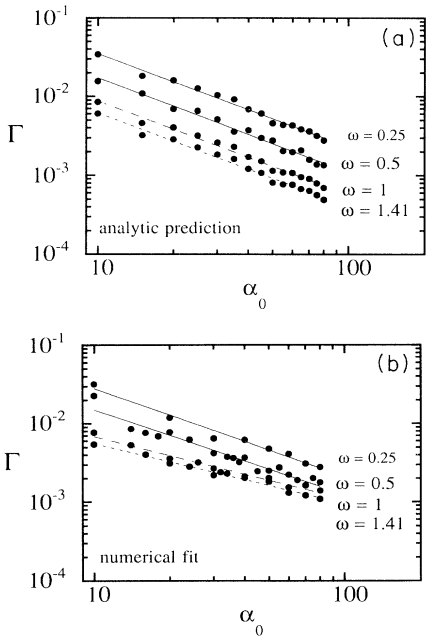

FIG. 7. Comparison between the analytical prediction and the numerical result. Both drawings represent the ground-state decay rate Γ vs the electron's classical excursion amplitude α_0 in atomic units, for four different values of the laser frequency, $\omega=0.25$, 0.50, 1, and 1.41 a.u. Dots in (a) show the results of the analytical prediction (21) at the same laser intensities studied in Fig. 6. They allow a reasonably good linear fit. (b) is a repetition of the numerical results (dots) with the corresponding linear fit suggested from (18).

V. CONCLUSIONS

We have analyzed the behavior of the ground-state decay in the ionization-suppression regime, in the Kramers-Henneberger frame. We have been working with square pulses and with the atom initially prepared in the Kramers-Henneberger ground state corresponding to the pulse intensity, without considering the dynamics during the pulse turn-on. Numerical computations show that for high intensities, but for frequencies close to the ionization potential, the decay is nearly purely exponential and slow. This allows one to identify a unique rate associated with each process. This rate has been compared with the analytical expression developed by Grozdanov, Krstic, and Mittleman [15], and qualitatively good agreement has been found.

ACKNOWLEDGMENTS

We thank J. H. Eberly for very interesting comments and suggestions. Support from the Spanish Dirección General de Investigación Científica y Tecnológica (Contract No. PB 89 0319 C0301) and from NATO (Contract No. CRG 900352) is acknowledged.

*Also at Max-Planck-Institut für Quantenoptik, D-8046 Garching, Germany.

[1] Q. Su, J. H. Eberly, and J. Javanainen, Phys. Rev. Lett. **64**, 862 (1990).
[2] Q. Su and J. H. Eberly, J. Opt. Soc. Am. B **7**, 564 (1990).
[3] Q. Su and J. H. Eberly, Phys. Rev. A **43**, 2474 (1991).
[4] J. H. Eberly and Q. Su, in *Multiphoton Processes,* edited by G. Mainfray and P. Agostini (CEA, Saclay, 1991), p. 81.
[5] V. C. Reed, P. L. Knight, and K. Burnett, Phys. Rev. Lett. **67**, 1415 (1991).
[6] K. Burnett, P. L. Knight, B. R. M. Piraux, and V. C. Reed, Phys. Rev. Lett. **66**, 301 (1991).
[7] V. C. Reed and K. Burnett, Phys. Rev. A **43**, 6217 (1991).
[8] J. Grochmalicki, M. Lewenstein, and K. Rzazewski, Phys. Lett. **66**, 1038 (1991).
[9] K. C. Kulander, K. J. Shafer, and J. L. Krause, Phys. Rev. Lett. **66**, 2601 (1991).
[10] K. C. Kulander, K. J. Schafer, and J. L. Krause, in *Multiphoton Processes* (Ref. [4]), p. 119.
[11] M. V. Fedorov and A. M. Movsesian, J. Opt. Soc. Am. B **6**, 928 (1989).
[12] J. Parker and C. R. Stroud, Jr., Phys. Rev. A **41**, 1602 (1990).
[13] R. Grobe and C. K. Law, Phys. Rev. A **44**, R4114 (1991).
[14] M. Pont and M. Gavrila, Phys. Rev. Lett. **65**, 2362 (1990).
[15] T. P. Grozdanov, P. S. Krstic, and M. H. Mittleman, Phys. Lett. A **149**, 144 (1990).
[16] J. Mostowski and J. H. Eberly, J. Opt. Soc. Am. B **8**, 1212 (1991).
[17] M. Pont, Phys. Rev. A **44**, 2152 (1991).
[18] R. R. Jones and P. H. Bruksbaum, Phys. Rev. Lett. **67**, 3215 (1991).
[19] J. I. Gersten and M. H. Mittleman, J. Phys. B **9**, 2561 (1976).
[20] M. Gavrila and J. Z. Kaminsky, Phys. Rev. Lett. **52**, 613 (1984).
[21] M. Gavrila, in *Fundamentals of Laser Interactions,* edited by F. Ehlotzky (Springer-Verlag, Berlin, 1985), p. 1.
[22] H. A. Kramers, *Collected Scientific Papers* (North-Holland, Amsterdam, 1956), p. 262.
[23] W. C. Henneberger, Phys. Rev. Lett. **21**, 838 (1968).
[24] C. Y. Tang, H. C. Bryant, P. G. Harris, A. H. Mohagheghi, R. A. Reeder, H. Sharifian, H. Tootoonchi, C. R. Quick, J. B. Donahue, S. Cohen, and W. W. Smith, Phys. Rev. Lett. **66**, 3124 (1991).
[25] S. Geltman, J. Phys. B **10**, 831 (1977).
[26] A. Sanpera and L. Roso-Franco, J. Opt. Soc. Am. B **8**, 1568 (1991).
[27] A. Sanpera, Ph. D. thesis, Universitat Autonoma de Barcelona, 1992.